World Journal of Gastroenterology

Online Submissions: http://www.wjgnet.com/1007-9327office
wjg@wjgnet.com
doi:10.3748/wjg.v18.i4.309

World J Gastroenterol 2012 January 28; 18(4): 309-322
ISSN 1007-9327 (print) ISSN 2219-2840 (online)

ORIGINAL ARTICLE

Embryonic hepatocyte transplantation for hepatic cirrhosis: Efficacy and mechanism of action

Wen-Ting Bin, Li-Mei Ma, Qing Xu, Xiao-Lin Shi

Wen-Ting Bin, Qing Xu, Xiao-Lin Shi, Laboratory of Reproductive Biology, Department of Histology and Embryology, School of Basic Medical Sciences, Capital Medical University, Beijing 100069, China
Li-Mei Ma, Department of Histology and Embryology, Kunming Medical University, Kunming 650031, Yunnan Province, China
Author contributions: Bin WT performed the majority of experiments and wrote the manuscript; Shi XL designed the research and revised the manuscript; Ma LM provided the animal models and performed parts of experiments; Xu Q performed B-ultrasound and data analysis.
Correspondence to: Xiao-Lin Shi, Supervisor of MD candidates, Laboratory of Reproductive Biology, Department of Histology and Embryology, School of Basic Medical Sciences, Capital Medical University, Beijing 100069, China. shixl.good@163.com
Telephone: +86-10-83911448 Fax: +86-10-83911450
Received: April 21, 2011 Revised: July 14, 2011
Accepted: July 21, 2011
Published online: January 28, 2012

Abstract

AIM: To investigate the efficacy and mechanism of action of allogeneic embryonic hepatocyte transplantation for the treatment of hepatic cirrhosis.

METHODS: Rat embryonic hepatocytes were characterized by examining cell markers. Wistar rats with CCl_4-induced cirrhosis were randomly divided into two groups: a model group receiving continuous CCl_4, and a cell transplantation group receiving continuous CCl_4 and transplanted with embryonic fluorescent-labeled hepatocytes. In addition, a normal control group was composed of healthy rats. All rats were sacrificed after 2 wk following the initiation of the cell transplant. Ultrasound, pathological analyses and serum biochemical tests were used to evaluate the efficacy of embryonic hepatocyte transplantation. To analyze the recovery status of cirrhotic hepatocytes and the signaling pathways influenced by embryonic hepatocyte transplantation, real-time polymerase chain reaction was performed to examine the mRNA expression of stellate activation-associated protein (STAP), c-myb, α smooth muscle actin (α-SMA) and endothelin-1 (ET-1). Western blotting and immunohistochemistry were employed to detect α-SMA and ET-1 protein expression in hepatic tissues.

RESULTS: Gross morphological, ultrasound and histopathological examinations, serum biochemical tests and radioimmunoassays demonstrated that hepatic cirrhosis was successfully established in the Wistar rats. Stem cell factor receptor (c-kit), hepatocyte growth factor receptor (c-Met), Nestin, α fetal protein, albumin and cytokeratin19 markers were observed in the rat embryonic hepatocytes. Following embryonic hepatocyte transplantation, there was a significant reversal in the gross appearance, ultrasound findings, histopathological properties, and serum biochemical parameters of the rat liver. In addition, after the activation of hepatic stellate cells and STAP signaling, α-SMA, c-myb and ET-1 mRNA levels became significantly lower than in the untreated cirrhotic group ($P < 0.05$). These levels, however, were not statistically different from those of the normal healthy group. Immunohistochemical staining and Western blot analyses revealed that α-SMA and ET-1 protein expression levels in the transplantation group were significantly lower than in the untreated cirrhotic group, but being not statistically different from the normal group.

CONCLUSION: Transplantation of embryonic hepatocytes in rats has therapeutic effects on cirrhosis. The described treatment may significantly reduce the expression of STAP and ET-1.

Key words: Embryonic hepatocytes; Cirrhosis; Stellate activation-associated protein; Endothelin-1; Cell transplantation

Peer reviewer: Shashi Bala, PhD, Post Doctoral Associate, Department of Medicine, LRB 270L, 364 Plantation street, UMass Medical School, Worcester, MA 01605, United States

Bin WT, Ma LM, Xu Q, Shi XL. Embryonic hepatocyte transplantation for hepatic cirrhosis: Efficacy and mechanism of action. *World J Gastroenterol* 2012; 18(4): 309-322 Available from: URL: http://www.wjgnet.com/1007-9327/full/v18/i4/309.htm DOI: http://dx.doi.org/10.3748/wjg.v18.i4.309

INTRODUCTION

Clinical studies of liver cell transplantation are primarily performed with adult hepatocytes and liver stem cells[1]. Adult hepatocytes are highly differentiated cells and cannot produce sufficient and sustained biological effects[2,3]. However, *in vitro* proliferation of liver stem cells allows for the generation of a sufficient number of cells to be used in clinical practice[4]. Following transplantation, liver stem cells continue to proliferate and may play an important role in liver regeneration[5,6].

There are currently several types of liver stem cells used in experimental research to treat cirrhosis, including adult liver stem/progenitor cells from the liver portal canal, which are activated and differentiate into hepatic oval cells following severe liver damage[7,8]. Other types of liver stem cells include embryonic hepatocytes[9,10], bone marrow/hematopoietic stem cells[11-16], and embryonic stem cells[17-19].

Early embryonic hepatocytes are self-renewing progenitor cells with the capacity to differentiate into adult hepatocytes and bile duct cells[20]. On embryonic days (E) 16 and 17, rat hepatic stem cells begin to differentiate. On E16, the gene expression profiles of rat embryonic liver epithelial cells change abruptly and become similar to those of mature cells; at this point, the bi-differentiation potential of these cells is significantly reduced[21]. On E9.5-15 in rats, most hepatocytes are liver stem cells, which possess potent proliferative capacity as compared with adult hepatocytes. After transplanted into injured livers, these cells can improve liver function and reduce animal mortality[22,23]. To investigate the effects of allogeneic embryonic hepatocyte transplantation on hepatic cirrhosis and the associated mechanisms of action, we utilized E15 rat hepatocytes as seed cells. The results presented here provide a theoretical and experimental framework for future studies of embryonic liver stem cell transplantation for the treatment of hepatic cirrhosis.

MATERIALS AND METHODS

Materials

Experimental animals: One hundred adult female Wistar rats and 6 male rats were purchased from the Specific Pathogen Free Grade Animal Department, Peking Union Medical College.

Primary reagents: Rabbit anti-human albumin (ALB) antibody and rabbit anti-rat cytokeratin 19 (CK19) antibodies were purchased from Beijing Gene Biology (Beijing, China). The rabbit anti-human α-fetoprotein (AFP) polyclonal antibody, the PV-6001 immunohistochemistry kit, PV-9003 immunohistochemistry kit and the chromogenic kit were purchased from Beijing Zhongshan Biology (Beijing, China). The rabbit anti-human/mouse/rat stem cell factor receptor (c-kit) antibody, the rabbit anti-human/mouse/rat hepatocyte growth factor receptor (c-Met) antibody, rabbit anti-human/mouse/rat Nestin antibodies were purchased from Wuhan Boster Biology (Wuhan, China). Percoll centrifugal liquid was purchased from Beijing Kehaijunzhou Bitechnology (Beijing, China). Collagenase type Ⅳ was purchased from Beijing Tianlai Biotech. Co. (Beijing, China). The rabbit anti-human/mouse/rat α smooth muscle actin (α-SMA) polyclonal antibody (ab66133) was purchased from Abcam (Cambridge, United Kingdom), the goat anti-human/mouse/rat endothelin-1 (ET-1) polyclonal antibody was purchased from Santa Cruz Biotechnology (California, United States), the biotinylated goat anti-rabbit immunoglobulin G (IgG) and anti-goat IgG antibodies were purchased from Beijing Zhongshan Biology (Beijing, China). β-actin was purchased from Santa Cruz Biotechnology (California, United States). The Power SYBR Green polymerase chain reaction (PCR) Master mix was purchased from ABI (California, United States), the M-MLV, dNTP Mix and Oligo (dT15) were purchased from Promega Corporation (Wisconsin, United States), and the Taq enzyme was purchased from TIANGEN (Beijing, China). Primers for stellate activation-associated protein (STAP), c-myb, α-SMA and ET-1 were purchased from Invitrogen Corporation (California, United States) and were synthesized by Beijing GENELIFE Biotech Co., Ltd (Beijing, China).

Experimental methods

Experimental animals: Females and male rats (2 females/1 male) were housed together overnight. Female vaginal smears were examined the following morning. The day when the sperm was detected was defined as day 0 of the pregnancy. Pregnant female rats at E15 were used to isolate embryonic hepatocytes.

Isolation of embryonic hepatocytes: The hepatocyte suspension was prepared using the enzymatic digestion method, and the hepatocytes were separated using Percoll gradient centrifugation. Percoll and a 9% NaCl solution were mixed at a ratio of 9:1. This solution was then diluted with D-F12 culture medium to 50%, 70% and 90% gradient centrifugation solutions. Each dilution of Percoll solution (5 mL) was added sequentially into a centrifuge tube, and the cell suspension was placed on the top of these solutions. The tube was centrifuged at 4330 *g* for 30 min at 4 ℃. The cells between the 50% and 70% Percoll layers were carefully removed and washed twice with Hank's balanced salt solution by centrifuging at 719 *g* and 4 ℃. The supernatant was discarded, and culture medium was added to the tube to a final volume of 1 mL. Cells

were counted using trypan blue after being re-suspended in the medium. Following calculation of the cell density, 2 × 10^6/mL cells were cultured in a 25-mm^2 flask.

***In vitro* culture of embryonic hepatocytes:** The flask was placed in a 37 ℃ incubator filled with 50 mL/L carbon dioxide. The D-F12 culture solution contained 15% fetal bovine serum (FBS), and the medium was replaced every 24 h. Cells were microscopically analyzed for growth and proliferation status, and the number of colonies was recorded.

Identification of colonies: Colonies were marked with a variety of liver stem cell markers using the two-step immunoperoxidase method. The analyzed markers included ALB (1:2000), AFP, c-kit, c-Met, Nestin and CK19 (all 1:1000).

Experimental groups: The Wistar rats were randomly divided into a cirrhotic group (n = 50) and a normal control group (n = 10). In the normal control group, olive oil was injected subcutaneously into the abdomen. In the cirrhotic group, 50% CCl_4 in olive oil was injected subcutaneously into the abdomen; the first four and final four doses were 0.5 mL/100 g body weight, and the other doses were 0.3 mL/100 g body weight. The 50% CCl_4 solution was injected every four days for a total of 15 injections. A 10% ethanol solution, which was prepared with white wine and distilled water, constituted the only liquid drank by the rats in the cirrhotic group.

After 63 d, the 24 surviving rats in the cirrhotic group (16 rats died during the induction of cirrhosis) were randomly divided into two groups: a control cirrhotic group (n = 12) and a cell transplantation group (n = 12). Rats in the control cirrhotic group received continuous CCl_4. In the cell transplantation group, rats were transplanted with E15 rat hepatocytes labeled with carboxyfluorescein diacetate and succinimidyl ester (CFSE) fluorescent molecules. CCl_4 was also continuously administered in this group. The rats were sacrificed 2 wk after the beginning of the transplantation treatment, and their serum was collected. A portion of liver tissue from the rats was used to prepare frozen and paraffin sections, and the remaining hepatic tissue was stored in liquid nitrogen for Western blotting and real time-PCR.

B-ultrasound image analysis: A solution of 0.5 mL/100 g chloral hydrate was used to anesthetize rats, and hair removal agents were used for skin preparation. Rats were immobilized on the operating table prior to the procedure. A small animal, high-resolution ultrasound system (Vevo 770TM) was used for image collection and analysis, and a PEF-704LA laparoscopic linear probe was used for abdominal exploration. The following ultrasound parameters were included: 2-D measurement of the portal vein and hepatic vein, Doppler imaging measurement of portal vein velocity (PVV) and hepatic vein velocity (HVV), echo intensity, the liver morphology and angle of the liver's blunt edge. SPSS13.0 software was used for statistical analyses following a completely randomized single-factor F test and paired t test.

Fluorescent labeling and tracking of E15 hepatocytes: CFSE was dissolved in dimethyl sulfoxide, and a 1-mmol/L CFSE solution was stored at -20 ℃. The stock solution was diluted to a 5 μmol/L working solution with phosphate buffer solution (PBS). Following a 20-min incubation with the CFSE working solution, fluorescence of the E15 hepatocytes was confirmed by excitation using a wavelength of 488 nm. The cells were digested with 0.25% trypsin, counted with trypan blue staining and diluted to 2 × 10^7 cells/0.5 mL.

Orthotopic liver transplantation of fluorescently-labeled embryonic hepatocytes: The rats were anesthetized with 0.5 mL/100 g chloral hydrate and immobilized on a surgical table. A 1.5-cm vertical incision on the right side of the abdomen was made under the xiphoid process to expose the liver. Using a 1-mL syringe, 0.5 mL of the labeled E15 hepatocyte suspension was slowly injected into the liver parenchyma. The abdomen was closed, and the rats were placed at ≥ 26 ℃ overnight.

Serum assay: Blood was taken from the abdominal aorta, and the following indicators were analyzed: total protein (TP), ALB, total bilirubin (TBil), alanine aminotransferase (ALT), and aspartate aminotransferase (AST). The levels of collagen type Ⅲ, AFP and ET-1 were determined by radioimmunoassays. SPSS13.0 software was used for statistical analysis using a completely randomized single-factor F test.

Histopathology: The rat livers were fixed in formalin for 48 h, paraffin embedded and sectioned into 4-μm thick slices for hematoxylin and eosin (HE) and van gieson (VG) staining.

Immunohistochemistry: Immunohistochemical staining of α-SMA, ET-1. Marker expression was examined using the two-step immunoperoxidase method. Briefly, after tissue sections were deparaffinized and rehydrated, sections were heated in a microwave for 10 min to enhance antigen retrieval. Slides were then incubated for 10 min with 3% H_2O_2 to inactivate endogenous peroxidase activity. Primary antibodies (rabbit anti-human/mouse/rat α-SMA polyclonal antibody, 1:50; goat anti-human/mouse/rat ET-1 polyclonal antibody, 1:50) were applied and incubated overnight at 4 ℃. The appropriate secondary antibody (biotinylated goat anti-rabbit IgG, 1:200; anti-goat IgG antibody, 1:200) was applied for 40 min, and 3,3'-diaminobenzidine was used as a chromogen. Negative controls were performed for each antibody using PBS instead of the primary antibody.

Immunohistochemical staining analysis: Immunohistochemical staining of paraffin-embedded liver sections was analyzed with a Leica Q500 IW Imaging Worksta-

Table 1 Primer sequences used for real-time polymerase chain reaction

Gene	Forward primer	Reverse primer	Segment length
STAP	AGTCCTCAGCTGCGGAAACA	AGCGCGAGCACAGAGGATAC	100 bp
α-SMA	CGGGCTTTGCTGGTGATG	GCTGTCCTTTTGGCCCATT	100 bp
C-myb	CCATCCAGAGACATTATAACGATGA	CTGTCCCTTCAGTTCGTTCTCTGT	100 bp
ET-1	GACCACAGACCAAGGGAACAG	TGGCATGGCCGAACTCAT	100 bp
β-actin	CATTGCTGACAGGATGCAGAAG	GAGCCACCAATCCACACAGAGT	100 bp

STAP: Stellate activation-associated protein; SMA: Smooth muscle actin; ET: Endothelin.

tion. The average optical density was calculated in image analysis. For quantitative analyses, several fields were selected in each slice using a micro-camera (Magnification: 10 × 10), and the images were transferred to a computer. The position of positive staining was first observed under low magnification, and the optical density values were measured using a high power (Magnification: 10 × 20). Five high-power fields of each specimen were randomly selected, and their average optical density value was calculated. SPSS13.0 software was used for the statistical analysis following a completely randomized single-factor *F* test.

Western blotting: Liver tissue samples and cells were lysed in ice-cold RIPA buffer supplemented with protease inhibitors. Whole cell lysates were obtained by subsequent centrifugation at 14 000 r/min for 10 min at 4 ℃. Protein concentrations were determined using the Bradford protein assay with bovine serum albumin as a standard. Twenty-five micrograms of protein extracts were separated using 10% sodium dodecyl sulfate-polyacrylamide gel electrophoresis and were transferred to a nitrocellulose membrane. Membranes were blocked with a 7.5% solution of nonfat dry milk dissolved in a Tris-HCl-buffered solution (TBS, pH 7.5) and were then probed with a primary antibody (rabbit anti-human/mouse/rat α-SMA polyclonal antibody, 1:50; goat anti-human/mouse/rat ET-1 polyclonal antibody, 1:50). Membranes were subsequently washed with TBST (TBS, 0.1% Tween 20) and exposed for 45 min at room temperature to the appropriate secondary antibody (anti-goat IgG antibody, 1:5000; anti-rabbit IgG antibody, 1:5000). Staining was detected using chemiluminescence followed by autoradiographic and densitometric analyses. Experiments were performed at least 3 times, and similar results were obtained for each replicate.

Real-time PCR: RNA from liver tissue was extracted using TRIzol. First-strand cDNA was reversely transcribed (RT) from 1 μg of total RNA using Oligo (dT) 15 primers and a M-MLV reverse transcriptase. The primers were designed based on gene sequence data from GenBank. Primer sequences used for real-time PCR are shown in Table 1. Real-time PCR was performed using an ABI Prism 7900HT Sequence Detection System (SDS). Triplicate reactions of each sample were performed in a 96-well plate using SDS instrumentation for 40 cycles. Real-time PCR amplifications were carried out using 2 μL cDNA, 12 μL 2 × SYBR Green PCR Master Mix, 0.3 μL primers (forward/reverse, 15 pmol/μL), and 10.4 μL H_2O for a final reaction volume of 25 μL. Real-time PCR cycling parameters were 50 ℃ for 2 min, 95 ℃ for 10 min, followed by 40 cycles of 95 ℃ for 15 s, 60 ℃ for 1 min, 95 ℃ for 15 s, 60 ℃ for 15 s and 95 ℃ for 15 s.

Data were analyzed using SDS2.2 software. The relative quantities of the target genes were normalized against the expression of β-actin[24]. The following formulas were used for RT-PCR data analysis: △Ct = Ct value of the target gene - Ct value of the normalization gene (the reference gene); quantity of the experimental group = 2-△Ct of the experimental group; quantity of the control group = 2-△Ct of the control group; quantity (relative expression levels) = quantity of the experimental group /quantity of the control group. After the expression of each gene in the normal control group was normalized to 1, the relative 2-ΔΔCt values for each gene in the untreated cirrhotic and the cell transplantation groups were calculated.

RESULTS

In vitro culture and identification of isolated cells

The primary fetal hepatocytes became adherent approximately 5 h into the culture period, and spheres formed on day 2 (Figure 1A). Spheres had a round or oval homogeneous morphology, and round or oval nuclei. Microscopic analysis revealed that the adherent cells grew in a monolayer and had a clear cell boundary (Figure 1B). Cells were round or polygonal and were arranged in neat rows. In addition, the cells had abundant cytoplasm and round nuclei. However, a small number of fibroblasts were observed within the cultures. Following a few days in culture, approximately half of the clones gradually grew into sheets and merged with one another or gradually differentiated (Figure 1C). In a 25-mm^2 flask, the peak number of cell colonies (> 4000 colonies) appeared on day 2 into the culture period. Most cells isolated from the 50% Percoll sample were not adherent, and a few gradually died over the course of the culture period.

Immunohistochemical staining revealed that most liver stem cell-specific markers, including c-kit (Figure 2A), c-Met (Figure 2B), Nestin (Figure 2C), AFP (Figure 2D), ALB (Figure 2E) and CK19 (Figure 2F), were expressed in the cell colonies on day 2 of culture.

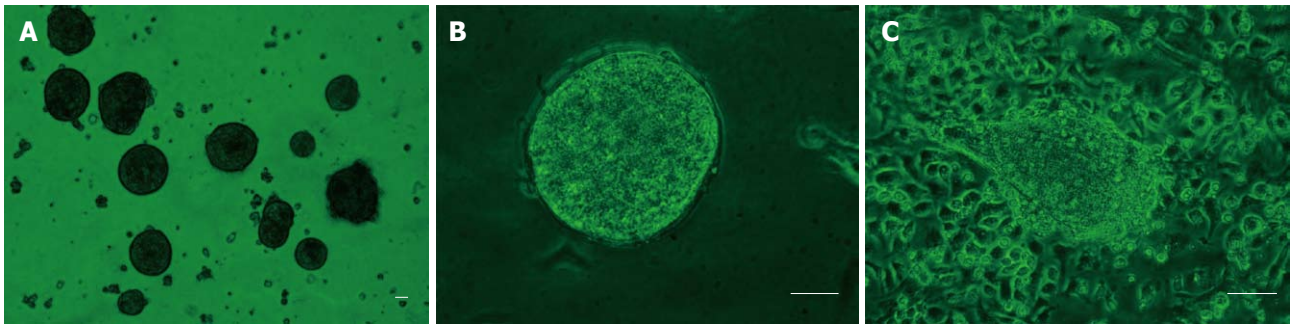

Figure 1 E15 rat hepatocytes *in vitro*. A: E15 rat hepatocytes 2 d after cell inoculation; B: E15 rat hepatocytes 2 d following cell inoculation; C: Differentiation of rat embryonic hepatocytes. Scale bars: 20 μm.

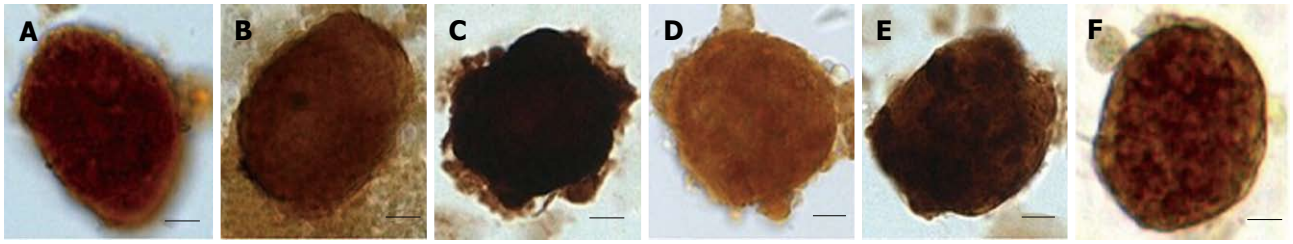

Figure 2 Immunohistochemistry staining of E15 rat hepatocytes. A: c-kit-positive colony; B: c-Met-positive colony; C: Nestin-positive colony; D: α-fetoprotein-positive colony; E: Albumin-positive colony; F: Cytokeratin 19-positive colony. Scale bars: 20 μm.

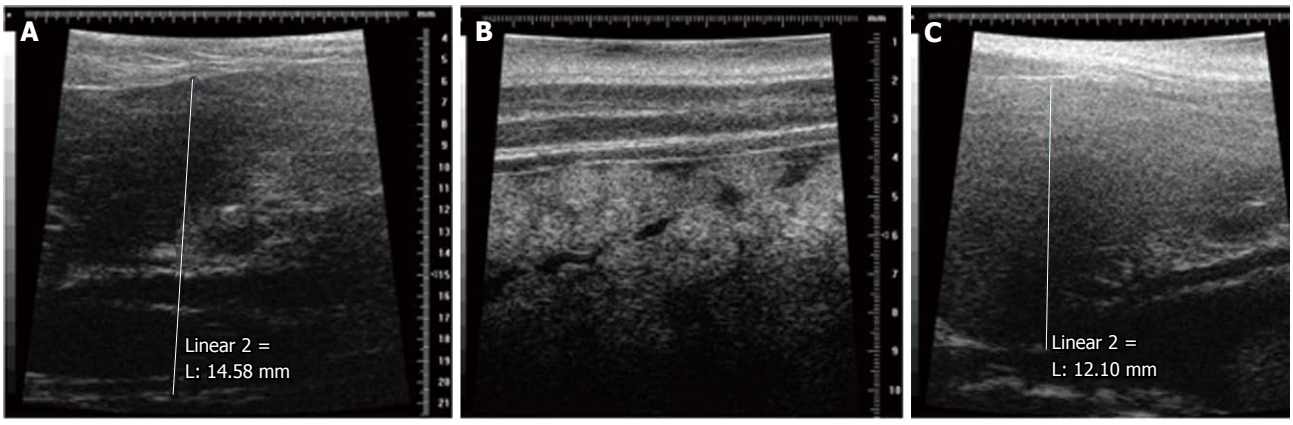

Figure 3 Parameters of ultrasound examination. A: Livers exhibit a smooth capsule, sharp edges, clear vascular texture and uniform echoes in the normal control group; B: Livers from rats of the untreated cirrhotic group exhibit uneven surfaces, blunt edges, unclear vascular texture and serrated and enhanced echoes with uneven distribution; C: In the transplantation group, rat livers exhibit a smooth capsule, smooth edges, clear vascular texture and even echo patterns.

Ultrasound examination

As shown in Figure 3A, ultrasound examination revealed that the livers of normal control rats had a smooth capsule, sharp edges, clear vascular texture and a uniform echo. In rats of the untreated cirrhotic group, however, livers had an uneven surface, blunt edges, unclear vascular texture, and serrated and enhanced echoes with uneven distributions (Figure 3B). No specific liver parenchymal lesions were observed in the untreated cirrhotic rats. Compared with the normal control group, the portal and hepatic veins in the untreated cirrhotic group were significantly widened ($P < 0.01$), and both PVV and HVV were significantly decreased ($P < 0.01$). Visible signs of ascites were observed in the untreated cirrhotic group. Ultrasound examination, therefore, revealed that livers of untreated cirrhotic rats were characterized by cirrhosis, portal hypertension, and the presence of ascites.

In the cell transplantation group, rat livers had a smooth capsule, smooth edges, clear vascular texture and even echo patterns (Figure 3C). Compared with the normal control group, the portal and hepatic veins were not obviously enlarged ($P > 0.05$, Table 2). The portal and hepatic veins were significantly narrower than those of rats in the untreated cirrhotic group ($P < 0.01$). PVV and HVV were decreased compared with the velocity in the normal control group ($P = 0.03$ and $P < 0.01$, respectively), but being higher than those observed in the untreated cirrhotic group (both $P < 0.01$). Findings and

Table 2 Results of ultrasound examination (mean ± SD, *n* = 10)

	Diameter of the major trunk of the portal vein (mm)	Hepatic vein diameter (mm)	PVV (mm/s)	HVV (mm/s)
Normal control group	1.545 ± 0.095	0.775 ± 0.058	117.319 ± 15.306	122.00 ± 14.553
Untreated cirrhotic group	2.518 ± 0.138[b]	1.378 ± 0.128[b]	53.663 ± 9.730[b]	56.817 ± 17.855[b]
Transplantation group	1.565 ± 0.135[d]	0.804 ± 0.096[d]	104.535 ± 11.654[a,d]	98.561 ± 15.955[b,d]

[a]$P < 0.05$, [b]$P < 0.01$ *vs* the normal control group; [d]$P < 0.01$ *vs* the untreated cirrhotic group. PVV: Portal vein velocity; HVV: Hepatic vein velocity.

Table 3 Effects of hepatocyte transplantation on ultrasound measurement (mean ± SD, *n* = 8)

	Diameter of the major trunk of the portal vein (mm)	Hepatic vein diameter (mm)	PVV(mm/s)	HVV (mm/s)
Before hepatocyte transplantation	2.571 ± 0.343	1.361 ± 0.136	67.441 ± 6.666	54.679 ± 17.453
After hepatocyte transplantation	1.575 ± 0.146	0.790 ± 0.137	100.968 ± 9.796	94.423 ± 5.207

PVV: Portal vein velocity; HVV: Hepatic vein velocity.

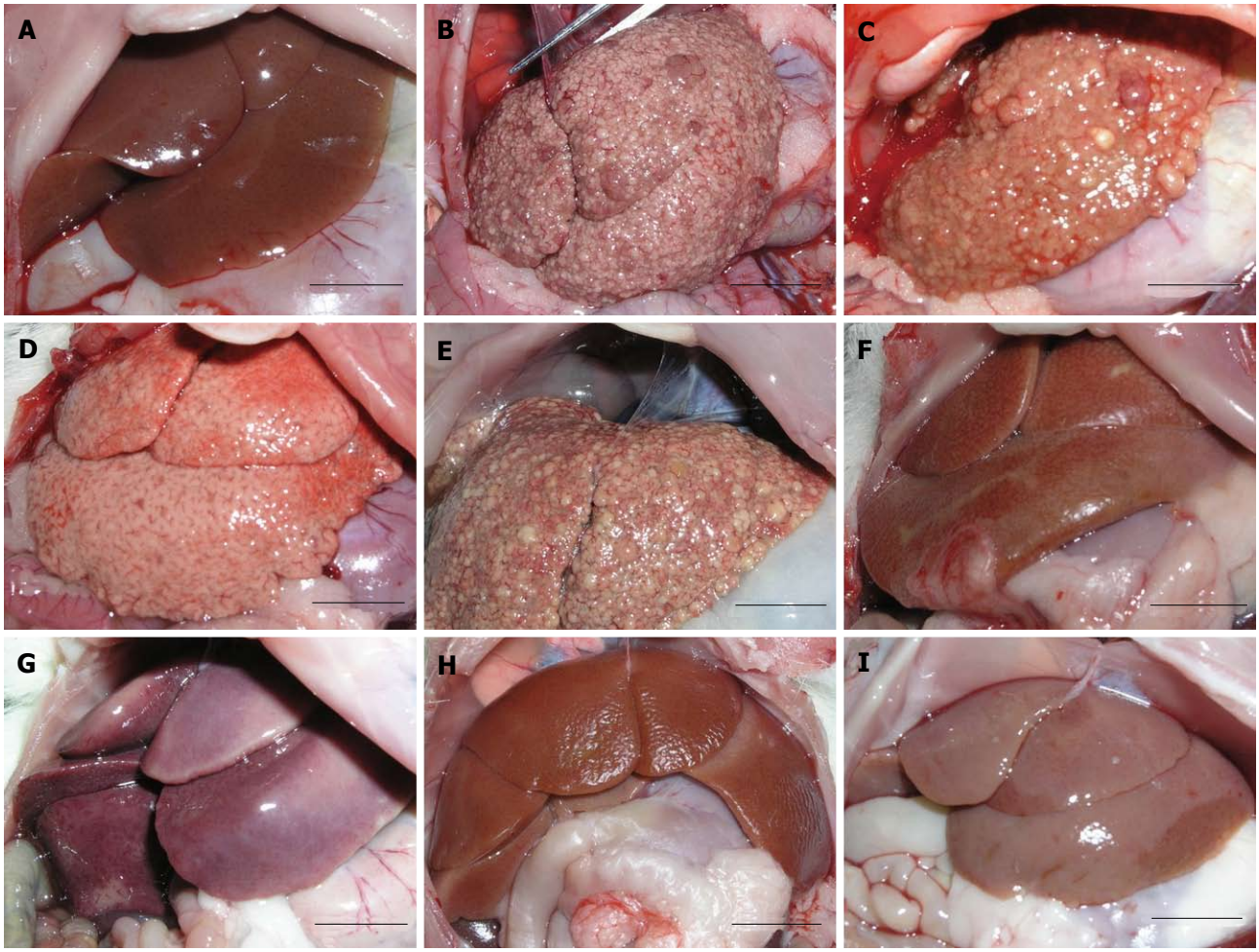

Figure 4 The appearance of rat livers. A: Normal control group; B-E: Untreated cirrhotic group; F-I: Transplantation group. Scale bars: 1 cm.

statistical results for each parameter of the ultrasound examination before and after liver transplantation (paired *t* test, $P < 0.01$) are shown in Table 3.

Pathological changes in rats with hepatic cirrhosis

The livers of normal control rats were dark red, elastic with a smooth surface, sharp edges and a soft texture (Figure 4A). However, the livers of rats in the untreated cirrhotic group had a hard texture, a brown or gray-brown appearance, diffuse surface nodules of variable sizes, blunt edges, uneven surfaces and were adhered to the adjacent organs (Figures 4B-E). The livers of rats in

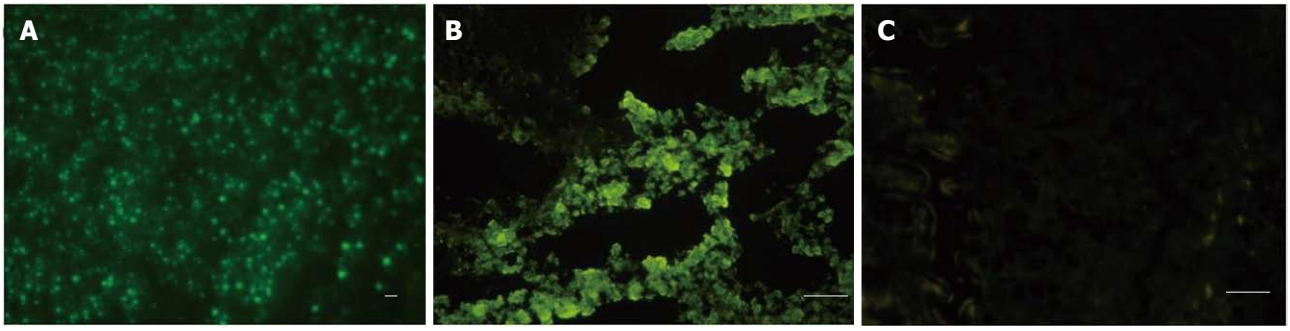

Figure 5 Tracking E15 hepatocytes. A: Using fluorescence microscopy, *in vitro* E15 hepatocytes demonstrated strong green fluorescence 2 d into the culture period with the carboxyfluorescein diacetate and succinimidyl ester fluorescent label; B: Cells in frozen liver tissue sections (2 wk following transplantation); scattered green fluorescent markers were observed; C: No fluorescent cells were observed in the frozen liver tissue sections of the untreated cirrhotic group. Scale bars: 20 μm.

Table 4 Effects of hepatocyte transplantation on serum biochemical tests (mean ± SD, *n* = 10)

	ALT (μmol/L)	AST (μmol/L)	TP (μmol/L)	ALB (μmol/L)	TBil (μmol/L)
Normal control group	22.297 ± 2.445	52.393 ± 32.356	61.984 ± 2.489	33.860 ± 1.102	2.015 ± 0.451
Untreated cirrhotic group	627.264 ± 113.580[b]	432.771 ± 100.330[b]	45.697 ± 2.646[b]	26.030 ± 1.282[b]	35.355 ± 9.587[b]
Transplantation group	86.623 ± 38.953[a,d]	158.284 ± 94.099[b,d]	56.174 ± 2.780[b,d]	31.330 ± 1.222[b,d]	1.957 ± 0.723[d]

[a]$P < 0.05$, [b]$P < 0.01$ *vs* the normal control group; [d]$P < 0.01$ *vs* the untreated cirrhotic group. ALT: Alanine aminotransferase; AST: Aspartate aminotransferase; TP: Total protein; ALB: Albumin; TBil: Total bilirubin.

Table 5 Effects of hepatocyte transplantation on serum marker levels (mean ± SD, *n* = 10)

	PⅢ (μg/L)	ET-1 (pg/mL)	AFP (ng/mL)
Normal control group	48.096 ± 5.010	45.459 ± 12.626	12.150 ± 11.430
Untreated cirrhotic group	92.954 ± 4.481[b]	132.192 ± 8.906[b]	12.099 ± 8.529
Transplantation group	54.023 ± 4.535[b,d]	42.383 ± 11.701[d]	61.315 ± 20.973[b,d]

[b]$P < 0.01$ *vs* the normal control group; [d]$P < 0.01$ *vs* the untreated cirrhotic group. ET: Endothelin; AFP: α-fetoprotein.

the transplantation group had a partially red appearance, soft texture, elasticity, sharp edges and smooth facets, similar to the normal control livers (Figures 4F-I).

Tracking E15 hepatocytes

Under fluorescence microscopy, E15 hepatocytes labeled *in vitro* with CFSE showed strong green fluorescence (Figure 5A). CFSE-labeled cells were transplanted into cirrhotic rat livers, and the livers were removed 2 wk after the transplantation. Scattered green fluorescent markers were observed in frozen tissue sections from these livers (Figure 5B); however, no fluorescent cells were observed in sections from the normal control or untreated cirrhotic rats (Figure 5C). These results suggest that embryonic hepatocytes labeled with CFSE *in vitro* are able to survive in the livers of cirrhotic rats.

Effects of hepatocyte transplantation on serum indicators

As shown in Table 4, ALT, AST and TBil levels in rats in the untreated cirrhotic group were much higher than in the normal control and cell transplantation groups. ALT and AST levels in the cell transplantation group were also slightly higher than in the normal control group ($P < 0.01$); however, no statistical differences in TBil levels were observed between the cell transplantation and normal control groups ($P > 0.05$). The TP and ALB levels of the model rats were lower than those in the cell transplantation group, which were also lower than the TP and ALB levels in the control group ($P < 0.01$).

PⅢ and ET-1 levels of rats in the untreated cirrhotic group were much higher than in the normal control or cell transplantation groups ($P < 0.01$, Table 5). PⅢ levels in rats with transplanted cells were higher than those observed in normal control rats ($P < 0.01$); however, no statistical difference in ET-1 levels was observed between the cell transplantation and normal control groups ($P > 0.05$). AFP levels in the cell transplantation group were much higher than in the control and untreated cirrhotic groups ($P < 0.01$); no statistical difference in AFP levels were observed between the control and untreated cirrhotic groups ($P > 0.05$).

Effects of hepatocyte transplantation on histopathology

Results of HE staining revealed that normal control rats exhibited typical liver lobules and orderly hepatic cords (Figure 6A). In contrast, livers from cirrhotic rats exhibited swollen hepatocytes, severe diffuse hydropic degeneration, and fatty degeneration. Some necrotic hepatocytes and pyknotic or dissolute nuclei were observed in the cirrhotic livers. The following abnormalities were also noted in the cirrhotic livers: remarkable expansions of the hepatic sinus and central vein; disorganization of the hepatic cord; apparent focal lymphocyte infiltration in the portal area; hyperplasia of the bile duct epithelia; brown pigmentation; diffuse hyperplasia of interstitial

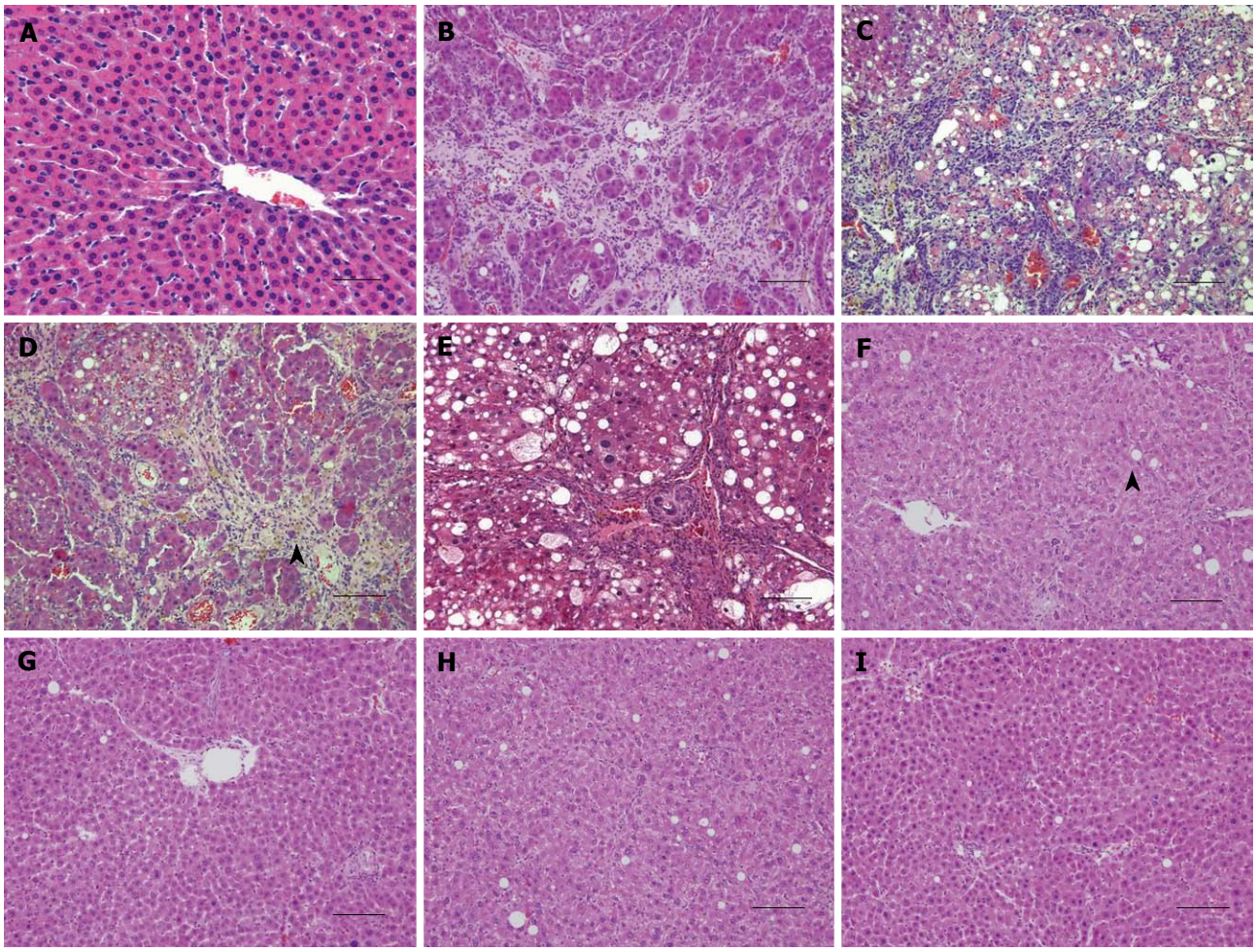

Figure 6 Hematoxylin and eosin staining of tissue slices from rat livers in each group. A: Normal liver lobules from the normal control group; B-E: Pseudo-lobules, fatty degeneration, necrotic hepatocytes, brown pigmentation (arrow) in livers from the untreated cirrhotic group; F-I: Sections from the cell transplantation group; a few cells have vacuoles (arrow), and liver lobules are present. Scale bars: 20 μm.

Table 6 Average optical density values (mean ± SD, *n* = 10)

	α-SMA	ET-1
Normal control group	0.140 ± 0.023	0.161 ± 0.022
Untreated cirrhotic group	0.602 ± 0.060[b]	0.523 ± 0.063[b]
Transplantation group	0.150 ± 0.031[d]	0.172 ± 0.021[d]

[b]$P < 0.01$ *vs* the normal control group; [d]$P < 0.01$ *vs* the untreated cirrhotic group. SMA: Smooth muscle actin; ET: Endothelin.

cells; noticeable fibrosis with septation; and formation of pseudo-lobules (Figures 6B-E). In the cell transplantation group, no pseudo-lobules or disorganized hepatic cords were detected, and the hepatocytes were similar to those in normal control rats. Although a small number of cells had vacuoles, most hepatocytes of the transplantation group had abundant cytoplasm (Figures 6F-I).

Depositions of collagen fibers were examined in VG-stained rat liver tissues. In the normal control group, rats had normal hepatic lobules. Hepatocytes were radially arranged around the central vein and no hyperplasia of the fibrous tissue was observed (Figure 7A). In the cirrhotic rats, the hepatic lobule was destroyed, and pseudo-lobules were surrounded by fibrous tissues (Figures 7B-E). The cell transplantation group exhibited noticeably less hyperplasia of the collagen fibers when compared with the untreated cirrhotic group (Figures 7F-I).

Immunohistochemical analysis

α-SMA expression was only observed in the vascular wall of normal rats; no significant expression was observed at other sites (Figure 8A). In untreated cirrhotic rats, α-SMA was primarily expressed in the periportal areas, fibrous septa, pseudo-lobules and hyperplastic fibers (Figure 8B). α-SMA expression in the cell transplantation group was observed in the periportal vascular wall while it was rarely detected in the periportal areas or fibrous septa (Figure 8C). The optical density (OD) values of α-SMA in the untreated cirrhotic group were much higher than in normal control or cell transplantation groups ($P < 0.01$, Table 6). No statistical difference was observed in the α-SMA OD values between the cell transplantation and normal control groups ($P > 0.05$).

Weak ET-1 expression was detected in a small number of sinusoid endothelial cells of the normal control rats (Figure 8D). In contrast, clear expression was ob-

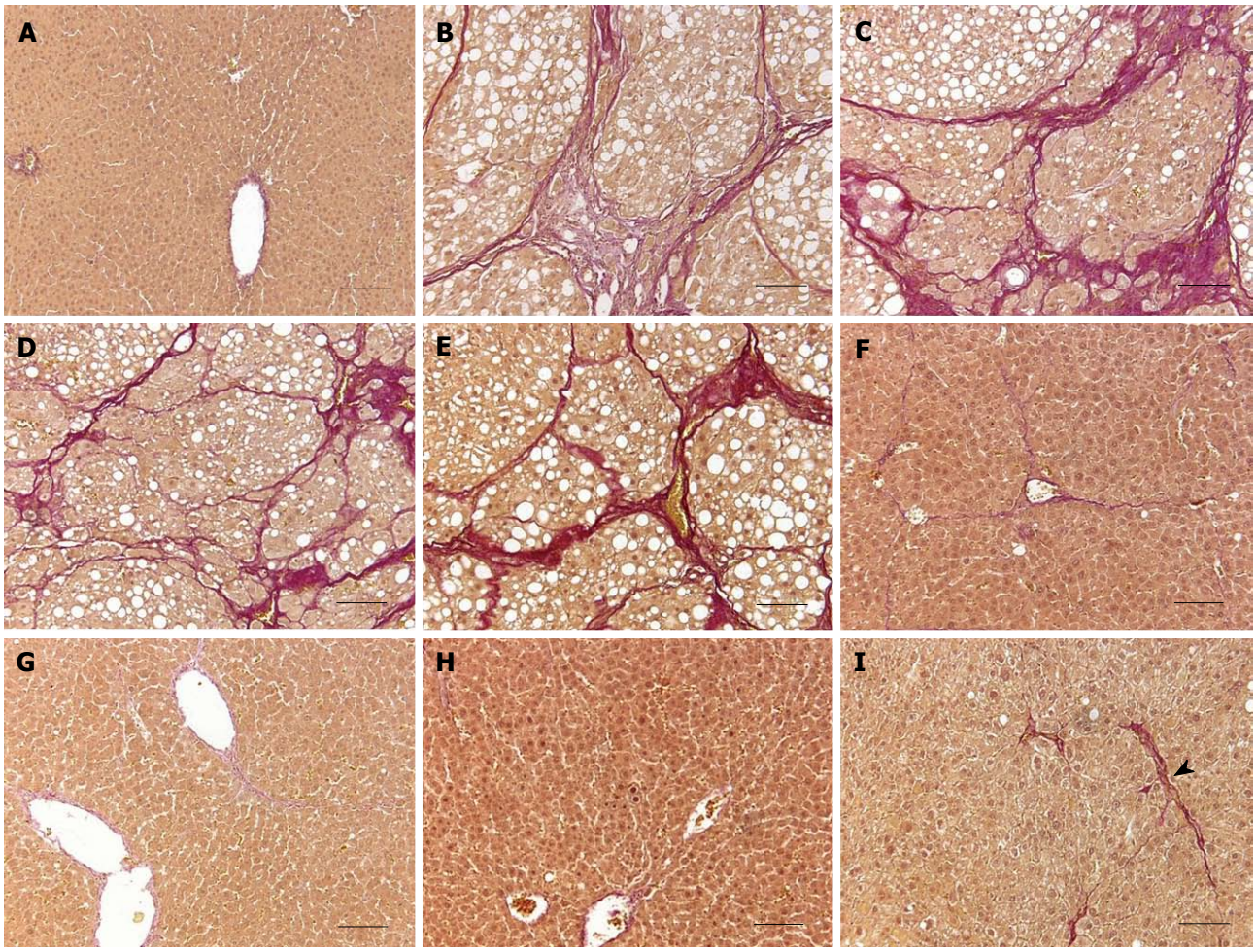

Figure 7 Van gieson staining of tissue slices from rat livers in each group. A: No hyperplasia of the fibrous tissue was observed in the normal control group; B-E: Pseudo-lobules were surrounded by fibrous tissues in livers from the untreated cirrhotic group; F-I: A few collagen fibers (arrow) were observed in livers from the transplantation group. Scale bars: 20 μm.

Table 7 Optical density values of Western blotting protein bands (mean ± SD, *n* = 3)

	α-SMA	ET-1
Normal control group	0.457 ± 0.055	0.593 ± 0.006
Untreated cirrhotic group	0.929 ± 0.036[b]	1.034 ± 0.112[b]
Transplantation group	0.502 ± 0.066[d]	0.607 ± 0.012[d]

[b]$P < 0.01$ *vs* the normal control group; [d]$P < 0.01$ *vs* the untreated cirrhotic group. SMA: Smooth muscle actin; ET: Endothelin.

served in the pseudo-lobules (Figure 8E) and fibrous septa (Figure 8F) of the untreated cirrhotic rats. In the cell transplantation group, ET-1 expression was only observed in the sinusoid endothelial cells (Figure 8G). The OD values of the untreated cirrhotic group were much higher than those of the normal control and cell transplantation groups ($P < 0.01$, Table 6). There was no significant difference in these values between the cell transplantation and control groups ($P > 0.05$).

Western blotting analysis

α-SMA and ET-1 expression levels in normal rat livers were extremely low (Figure 9). α-SMA and ET-1 protein was more highly expressed in the liver tissues of the untreated cirrhotic group than in the normal group. Additionally, the expression of α-SMA and ET-1 in rats treated with cell transplantation was significantly lower than that of the untreated cirrhotic group ($P < 0.01$). There was no statistically significant difference between the cell transplantation group and the control group ($P > 0.05$). The Western blotting optical density ratios are shown in Table 7.

Real-time PCR

After the expression of each gene in the normal control group was normalized to 1, the relative $2^{-\Delta\Delta Ct}$ value of each gene in the untreated cirrhotic and cell transplantation groups was calculated. Compared with the control group, the expression levels of STAP, c-myb, α-SMA and ET-1 were increased in the untreated cirrhotic group ($P < 0.01$). However, the expression levels of these mRNAs in rats of the cell transplantation group were significantly reduced when compared with the untreated cirrhotic group ($P < 0.01$) (Table 8). There was no statistically significant difference between the cell transplantation and

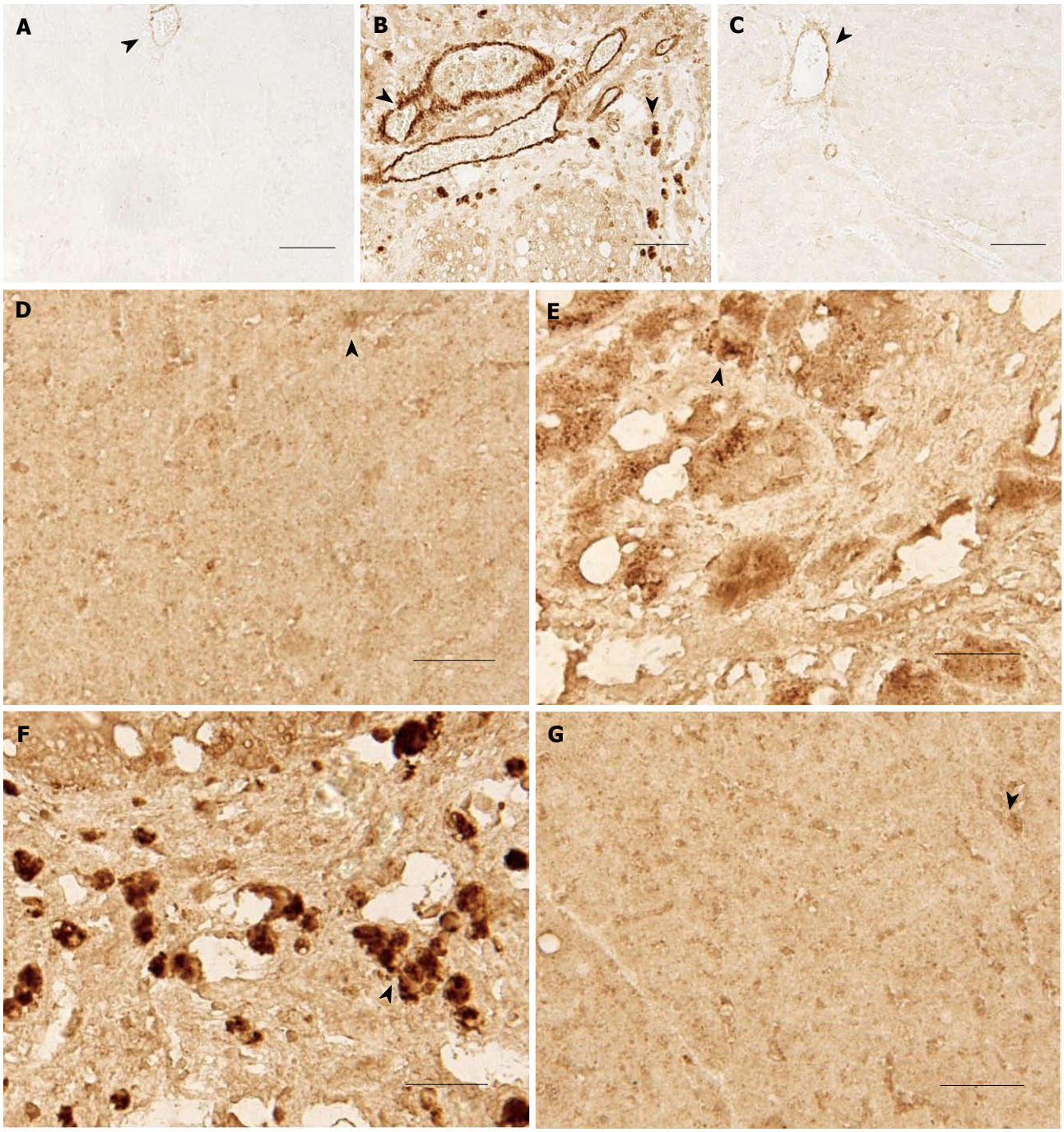

Figure 8 Immunohistochemical staining of rat livers in each group. A: α smooth muscle actin (α-SMA) expression (arrow) was only observed in the vascular wall of the normal group; B: α-SMA (arrow) was highly expressed in the periportal areas and fibrous septa of livers from the untreated cirrhotic group; C: The cell transplantation group exhibited noticeably weaker α-SMA (arrow) expression than the untreated cirrhotic group; D: Weak endothelin-1 (ET-1) (arrow) expression was detected in a few sinusoid endothelial cells of livers from the normal control group; E: Clear ET-1 expression (arrow) was observed in the pseudo-lobules of livers from the untreated cirrhotic group; F: Clear ET-1 (arrow) expression in the fibrous septa of livers from the untreated cirrhotic group; G: In the cell transplantation group, ET-1 (arrow) expression was only observed in the sinusoid endothelial cells. Scale bars: 20 μm.

control groups ($P > 0.05$).

DISCUSSION

There is no precise or unified definition for hepatic stem cells. In 1956, Farber *et al*[25] observed hepatic oval cells with a diameter of approximately 10 μm. These cells were shown to be able to differentiate into either hepatocytes or bile duct cells and were considered as liver stem cells[8,26,27]. It is well known that hepatic stem cells have unlimited proliferative capacity and the potential to differentiate into hepatocytes.

The morphology, phenotype and molecular expression profile of hepatic stem cells change dynamically in their degree of differentiation[28]. Due to the lack of specific markers, hepatic stem cells are principally identified

Table 8 Effects of embryonic hepatocyte transplantation in rats on different mRNA expression (mean ± SD, *n* = 9)

	STAP	c-myb	α-SMA	ET-1
Normal control group	1.000 ± 0.2667	1.000 ± 0.250	1.000 ± 0.2446	1.000 ± 0.3191
Untreated cirrhotic group	44.97 ± 19.40[b]	22.32 ± 5.536[b]	45.65 ± 11.98[b]	8.021 ± 1.191[b]
Transplantation group	1.133 ± 0.2222[d]	0.7143 ± 0.5714[d]	1.094 ± 0.1974[d]	1.010 ± 0.3298[d]

[b]$P < 0.01$ *vs* the normal control group; [d]$P < 0.01$ *vs* the untreated cirrhotic group. STAP: Stellate activation-associated protein; SMA: Smooth muscle actin; ET: Endothelin.

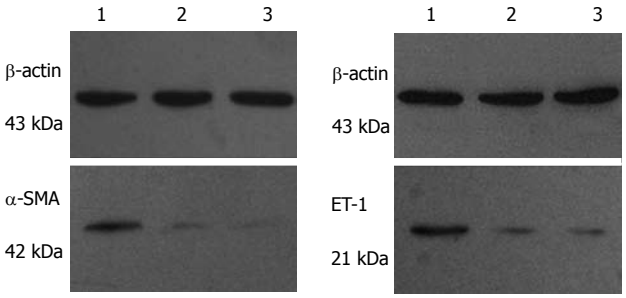

Figure 9 Western blotting analysis of α smooth muscle actin and endothelin-1 expression in liver tissues. Lane 1: The untreated cirrhotic group; Lane 2: The cell transplantation group; Lane 3: The normal control group. SMA: Smooth muscle actin. ET-1: Endothelin-1.

using their differentiation potentials. Hepatic stem cells with bi-potentiality can differentiate into hepatocytes and biliary duct epithelial cells and can be identified using antibodies for specific hepatocyte and biliary epithelial cell markers. Pack *et al*[29] reported that ALB specifically marks mature hepatocytes and that CK19 specifically marks bile duct epithelial cells[30]. Although AFP can be expressed in both embryonic hepatocytes and hepatic oval cells, AFP synthesis ceases upon differentiation and maturation of hepatocytes[31]. c-Met and Nestin are stem cell markers, and c-kit is a common epitope for hepatic and blood stem cells[32-35].

In this study, E15 hepatocytes were cultured *in vitro* and grew in a similar manner as stem cells, exhibiting colony-like growth with clear boundaries for each clone. Molecular characterization revealed that c-kit, c-Met, Nestin, AFP, ALB and CK19 were expressed in the majority of colony cells, suggesting that the majority of rat E15 hepatocytes were undifferentiated and bipotential. Because embryonic hepatocytes have a higher proliferative capacity, multiple differentiation potentials, and low immunogenicity, there is greater clinical value for embryonic hepatocytes than for mature hepatocytes in the treatment of liver injury due to chronic cirrhosis.

The use of CCl_4 and alcohol to induce and model cirrhosis has a high success rate, which is the reason why this technique is chosen for this study. Following the completion of this protocol, ultrasound examination and HE and VG staining of paraffin-embedded specimens revealed pathological changes indicative of hepatic cirrhosis. In addition, serum biochemical indicators were also abnormal, suggesting that hepatic cirrhosis was effectively induced.

Two weeks after E15 hepatocytes were transplanted into the cirrhotic rats, serum levels of ALT, TBil, type-Ⅲ procollagen and ET-1 were significantly reduced. However, serum ALB and TP were significantly increased, indicating that embryonic liver hepatocyte transplantation significantly improved the hepatic function of cirrhotic rats. This conclusion is particularly exemplified by the observed normalization of total bilirubin levels in treated cirrhotic rats. Serum AFP levels in the cell transplantation group were significantly higher than in the untreated cirrhotic group, suggesting that the biological activities of transplanted embryonic hepatocytes induced liver regeneration in cirrhotic rats. There was no significant difference in the ultrasound results between the cell transplantation and normal control groups; neither high portal vein pressure nor ascites were observed. Pathological results revealed that collagen fiber hyperplasia was significantly reduced in rats treated with liver cell transplantation. A small number of collagen fibers around the lobules were observed in treated livers, and the majority of hepatocytes in the lobules were morphologically normal. All these results demonstrate that rat embryonic hepatocyte transplantation significantly improves liver morphology and function in rats with hepatic cirrhosis. These cells also effectively inhibit hepatic necrosis and fibrosis and promote normal hepatocyte proliferation and function.

CCl_4 is a hepatotoxic compound that damages the liver *via* lipid peroxidation[36,37] and leads to intracellular calcium overload, resulting in fatty degeneration of hepatocytes. Continuous administration of CCl_4 in rats leads to hepatic necrosis. Moreover, CCl_4 may cause hepatocyte damage *via* its metabolism into CCl_3 radicals by cytochrome P450, resulting in the oxidation of unsaturated fatty acids and the production of lipid peroxides[38]. Lipid peroxidation can directly activate hepatic stellate cells (HSCs) and facilitate hepatocyte conversion to myofibroblasts. The latter cell type subsequently synthesizes extracellular matrix (ECM) proteins, leading to liver fibrosis[39].

The metabolites of alcohol, such as acetaldehyde, lactic acid, and reactive oxygen species (ROS), can stimulate oxidative stress and cytokine-mediated damage. ROS generated by alcohol metabolism in hepatocytes is also known to activate HSCs and to result in the production of large amounts of collagen[40,41]. Alcohol-induced hepatocyte apoptotic bodies can be phagocytosed by HSCs and Kupffer cells, resulting in HSC activation and ECM synthesis.

The combination of CCl_4 and alcohol induced hepat-

ic cirrhosis in rats in the current study. Although these two agents induced cirrhogenesis *via* distinct mechanisms, they ultimately converged on the key step of HSC activation. Under normal circumstances, HSCs are in a resting state. Following liver damage, however, HSCs are activated and transformed into myofibroblast-like cells, a transition characterized by the loss of cytoplasmic lipid droplets, morphological changes, and the expression of α-SMA and many cytokines and their receptors. These myofibroblast-like cells can proliferate and synthesize a variety of ECM proteins, primarily type- I and type-Ⅲ collagens. HSC activation plays an essential role in liver fibrosis and can cause excessive accumulations of ECM proteins in the liver, resulting in liver fibrosis and cirrhosis. In 2001, Kawada *et al*[42] described a novel protein in rat HSCs that is highly associated with HSC activation, namely STAP [also referred to as cytoglobin/STAP (Cygb/STAP)]. STAP is a cytoplasmic protein in HSCs and myofibroblasts, and both protein and mRNA levels are significantly up-regulated during HSC activation[42,43]. Kang *et al*[44] used the increased expression of STAP as an indicator of cirrhosis in the rat model of cirrhosis.

Our results demonstrate that STAP mRNA expression in the untreated cirrhotic rats was significantly higher than in control rats, indicating the HSC activation and the development of hepatic cirrhosis in untreated cirrhotic rats. CCl_4 and other pathogenic factors can lead to lipid peroxidation, the up-regulation of STAP-related signaling pathways, and HSC activation. Due to the peroxidative activities of STAP on hydrogen peroxide and lipid peroxides, increased expression of this gene can lower the peroxide levels and prevent hepatic fibrosis[42]. In the present study, STAP mRNA levels were much lower in the transplantation group than in the untreated cirrhotic group and were comparable to the normal control group. This result suggests that HSCs in the cell transplantation group were in a resting state and that STAP-related signaling pathways were inactive. Alternatively, transplanted embryonic hepatocytes may selectively induce activated HSCs to undergo apoptosis or inactivate HSCs. Therefore, cell transplantation treatment maintains HSCs in a resting state[45] and reverses hepatic cirrhosis in rats.

There are no definitive reports with respect to upstream regulators of STAP. *In vitro* experiments found that α-SMA can induce increased expression of STAP, but STAP is not regulated by IFN-γ, TGF-β, PDGF/BB, cAMP or cGME[42]. In the initial stages of HSC activation, the transcription factor c-myb is up-regulated. c-myb is a proto-oncogene, and its expression is growth-dependent; it is expressed at low levels in quiescent cells, and its expression is rapidly increased in exponentially dividing cells. c-myb can interact with α-SMA promoter regulatory elements and alter α-SMA expression. α-SMA is a microfilament protein with contractile properties and is widely distributed in muscle cells. It is also the cytoskeletal marker of HSC activation, and its increased expression may up-regulate STAP expression. In the present study, mRNA levels of c-myb, α-SMA and STAP were significantly increased in the untreated cirrhotic group but were much lower in the cell transplantation group. However, there was no significant difference between the normal control and the cell transplantation group. Similar results were observed in α-SMA protein expression levels. These findings suggest that the observed successful treatment of cirrhosis with embryonic hepatocyte transplantation is related to the activity of STAP-related signaling.

ET is the most powerful vasoconstrictor peptide in humans; it is also a damage-inducible factor produced during ischemia and hypoxia[46]. The occurrence and development of many chronic liver diseases, such as hepatic cirrhosis, are related to ET plasma and tissue levels. ET-1 is the most important member of the ET family and is one of the primary inducers of portal hypertension[47]. ET-1 catalyzes the phosphorylation of amino acid residues in many kinases through the G-protein complex-phospholipase C-protein kinase C signaling pathway. ET-1 thereby regulates gene expression and promotes HSC mitosis and the synthesis of collagen and matrix proteins[48]. After ET-1 binds to its receptor, endothelin receptor, it activates voltage-dependent calcium channels, promoting calcium influx and leading to vasoconstriction. HSC is considered one of the main sources of ET-1, which is involved in increased portal vein pressure and plays an important role in the regulation of blood flow in the liver. In the normal liver, ET-1 is primarily expressed in liver sinusoid endothelial cells; upon liver injury, however, ET-1 is primarily expressed in activated HSCs.

Contraction of the portal vein and sinusoid as a result of EF-1-induced HSC activation may be a significant event in cirrhogenesis, resulting in increased portal vein obstruction following liver fibrosis[49]. In the current study, serum and liver ET-1 levels were significantly higher in the untreated cirrhotic group when compared with the normal control and cell transplantation groups. Ultrasound results demonstrated that the untreated cirrhotic rats had a wider portal vein and reduced PVV. Rats in the cell transplantation group showed significant remission, suggesting that treatment of hepatic cirrhosis with embryonic hepatocytes is able to reduce ET-1 expression and modify various parameters of this pathway. The reduction in the portal vein pressure of the cell transplantation-treated cirrhotic group may indicate a remission of the portal hypertension caused by cirrhosis.

Significant therapeutic effects were observed in the treatment of hepatic cirrhosis using embryonic hepatocyte transplantation in rats. Transplanted embryonic hepatocytes significantly reduce c-myb, α-SMA and STAP expression, all of which are involved in HSC activation. This treatment also down-regulates the expression of ET-1, a vasoactive substance.

COMMENTS

Background

Hepatic cirrhosis is a terminal illness that can only be cured by a liver trans-

plant. Stem cells are capable of indefinite self-renewal and are able to generate other cell types *via* differentiation. Stem cell transplantation is the most promising therapy for hepatic cirrhosis. Embryonic hepatocytes are stem cells that have the capacity to proliferate and to differentiate into hepatocytes. These cells have a more promising clinical potential than adult hepatocytes for the treatment of liver injury due to chronic cirrhosis.

Research frontiers

Stem cell transplantation for the treatment of hepatic cirrhosis is far from application. The identification of the most effective stem cells and probe into their mechanisms of action have recently become a popular research topic.

Innovations and breakthroughs

The authors confirm the efficacy of embryonic hepatocyte transplantation for hepatic cirrhosis in rats by demonstrating reduced expression level of stellate activation-associated protein (STAP), α smooth muscle actin and endothelin-1. In addition, they initially revealed the mechanism of this therapy, which may be of significance for the treatment of hepatic cirrhosis.

Applications

Although it is far from clinical application, it is possible that embryonic hepatocyte transplantation will become a curative treatment for hepatic cirrhosis and other severe liver diseases. This study has laid a foundation for further experimental researches and clinical studies, and provided useful data for the treatment of cirrhosis.

Terminology

STAP is a protein expressed in hepatic stellate cells. Hepatocyte damage leads to increased STAP expression; therefore, STAP can be used as an indicator of cirrhosis in the rat cirrhosis model.

Peer review

This is a well-performed and comprehensive study. The authors show the effectiveness of embryonic stem cells to treat cirrhosis. Furthermore, the mechanism by which this protective effect is mediated has been elucidated.

REFERENCES

1 **Enns GM**, Millan MT. Cell-based therapies for metabolic liver disease. *Mol Genet Metab* 2008; **95**: 3-10
2 **Bilir BM**, Guinette D, Karrer F, Kumpe DA, Krysl J, Stephens J, McGavran L, Ostrowska A, Durham J. Hepatocyte transplantation in acute liver failure. *Liver Transpl* 2000; **6**: 32-40
3 **Muraca M**, Gerunda G, Neri D, Vilei MT, Granato A, Feltracco P, Meroni M, Giron G, Burlina AB. Hepatocyte transplantation as a treatment for glycogen storage disease type 1a. *Lancet* 2002; **359**: 317-318
4 **Suzuki A**, Nakauchi H, Taniguchi H. In vitro production of functionally mature hepatocytes from prospectively isolated hepatic stem cells. *Cell Transplant* 2003; **12**: 469-473
5 **Bae SH**. [Clinical application of stem cells in liver diseases]. *Korean J Hepatol* 2008; **14**: 309-317
6 **Zhang B**, Inagaki M, Jiang B, Miyakoshi M, Arikura J, Ogawa K, Kasai S. Effects of bone marrow and hepatocyte transplantation on liver injury. *J Surg Res* 2009; **157**: 71-80
7 **Petersen BE**, Grossbard B, Hatch H, Pi L, Deng J, Scott EW. Mouse A6-positive hepatic oval cells also express several hematopoietic stem cell markers. *Hepatology* 2003; **37**: 632-640
8 **Zhou H**, Rogler LE, Teperman L, Morgan G, Rogler CE. Identification of hepatocytic and bile ductular cell lineages and candidate stem cells in bipolar ductular reactions in cirrhotic human liver. *Hepatology* 2007; **45**: 716-724
9 **Tee LB**, Kirilak Y, Huang WH, Morgan RH, Yeoh GC. Differentiation of oval cells into duct-like cells in preneoplastic liver of rats placed on a choline-deficient diet supplemented with ethionine. *Carcinogenesis* 1994; **15**: 2747-2756
10 **Khan AA**, Habeeb A, Parveen N, Naseem B, Babu RP, Capoor AK, Habibullah CM. Peritoneal transplantation of human fetal hepatocytes for the treatment of acute fatty liver of pregnancy: a case report. *Trop Gastroenterol* 2004; **25**: 141-143
11 **Petersen BE**, Goff JP, Greenberger JS, Michalopoulos GK. Hepatic oval cells express the hematopoietic stem cell marker Thy-1 in the rat. *Hepatology* 1998; **27**: 433-445
12 **Yao P**. Stem cells and liver diseases. *Zhonghua Ganzangbing Zazhi* 2007; **15**: 219- 220
13 **Oh SH**, Witek RP, Bae SH, Zheng D, Jung Y, Piscaglia AC, Petersen BE. Bone marrow-derived hepatic oval cells differentiate into hepatocytes in 2-acetylaminofluorene/partial hepatectomy-induced liver regeneration. *Gastroenterology* 2007; **132**: 1077-1087
14 **Yagi K**, Kojima M, Oyagi S, Ikeda E, Hirose M, Isoda K, Kawase M, Kondoh M, Ohgushi H. [Application of mesenchymal stem cells to liver regenerative medicine]. *Yakugaku Zasshi* 2008; **128**: 3-9
15 **Yan L**, Han Y, Wang J, Liu J, He Y, Wang H, Fan D. Peripheral blood monocytes from the decompensated liver cirrhosis could migrate into nude mouse liver with human hepatocyte-markers expression. *Biochem Biophys Res Commun* 2008; **371**: 635-638
16 **Dai LJ**, Li HY, Guan LX, Ritchie G, Zhou JX. The therapeutic potential of bone marrow-derived mesenchymal stem cells on hepatic cirrhosis. *Stem Cell Res* 2009; **2**: 16-25
17 **Yamada T**, Yoshikawa M, Kanda S, Kato Y, Nakajima Y, Ishizaka S, Tsunoda Y. In vitro differentiation of embryonic stem cells into hepatocyte-like cells identified by cellular uptake of indocyanine green. *Stem Cells* 2002; **20**: 146-154
18 **Teratani T**, Yamamoto H, Aoyagi K, Sasaki H, Asari A, Quinn G, Sasaki H, Terada M, Ochiya T. Direct hepatic fate specification from mouse embryonic stem cells. *Hepatology* 2005; **41**: 836-846
19 **Cai J**, Zhao Y, Liu Y, Ye F, Song Z, Qin H, Meng S, Chen Y, Zhou R, Song X, Guo Y, Ding M, Deng H. Directed differentiation of human embryonic stem cells into functional hepatic cells. *Hepatology* 2007; **45**: 1229-1239
20 **Kruglov EA**, Jain D, Dranoff JA. Isolation of primary rat liver fibroblasts. *J Investig Med* 2002; **50**: 179-184
21 **Petkov PM**, Kim K, Sandhu J, Shafritz DA, Dabeva MD. Identification of differentially expressed genes in epithelial stem/progenitor cells of fetal rat liver. *Genomics* 2000; **68**: 197-209
22 **Nowak G**, Ericzon BG, Nava S, Jaksch M, Westgren M, Sumitran-Holgersson S. Identification of expandable human hepatic progenitors which differentiate into mature hepatic cells in vivo. *Gut* 2005; **54**: 972-979
23 **Machimoto T**, Yasuchika K, Komori J, Ishii T, Kamo N, Shimoda M, Konishi S, Saito M, Kohno K, Uemoto S, Ikai I. Improvement of the survival rate by fetal liver cell transplantation in a mice lethal liver failure model. *Transplantation* 2007; **84**: 1233-1239
24 **Livak KJ**, Schmittgen TD. Analysis of relative gene expression data using real-time quantitative PCR and the 2(-Delta Delta C(T)) Method. *Methods* 2001; **25**: 402-408
25 **Farber E**. Similarities in the sequence of early histological changes induced in the liver of the rat by ethionine, 2-acetylamino-fluorene, and 3'-methyl-4-dimethylaminoazobenzene. *Cancer Res* 1956; **16**: 142-148
26 **Strom S**, Fisher R. Hepatocyte transplantation: new possibilities for therapy. *Gastroenterology* 2003; **124**: 568-571
27 **Fougère-Deschatrette C**, Imaizumi-Scherrer T, Strick-Marchand H, Morosan S, Charneau P, Kremsdorf D, Faust DM, Weiss MC. Plasticity of hepatic cell differentiation: bipotential adult mouse liver clonal cell lines competent to differentiate in vitro and in vivo. *Stem Cells* 2006; **24**: 2098-2109
28 **Yovchev MI**, Grozdanov PN, Joseph B, Gupta S, Dabeva MD. Novel hepatic progenitor cell surface markers in the adult rat liver. *Hepatology* 2007; **45**: 139-149
29 **Pack R**, Heck R, Dienes HP, Oesch F, Steinberg P. Isolation, biochemical characterization, long-term culture, and phenotype modulation of oval cells from carcinogen-fed rats. *Exp Cell Res* 1993; **204**: 198-209

30 **Zaret KS**. Genetic programming of liver and pancreas progenitors: lessons for stem-cell differentiation. *Nat Rev Genet* 2008; **9**: 329-340

31 **Petersen BE**, Bowen WC, Patrene KD, Mars WM, Sullivan AK, Murase N, Boggs SS, Greenberger JS, Goff JP. Bone marrow as a potential source of hepatic oval cells. *Science* 1999; **284**: 1168-1170

32 **Crosby HA**, Hubscher SG, Joplin RE, Kelly DA, Strain AJ. Immunolocalization of OV-6, a putative progenitor cell marker in human fetal and diseased pediatric liver. *Hepatology* 1998; **28**: 980-985

33 **Suzuki A**, Zheng Y, Kondo R, Kusakabe M, Takada Y, Fukao K, Nakauchi H, Taniguchi H. Flow-cytometric separation and enrichment of hepatic progenitor cells in the developing mouse liver. *Hepatology* 2000; **32**: 1230-1239

34 **Tanimizu N**, Tsujimura T, Takahide K, Kodama T, Nakamura K, Miyajima A. Expression of Dlk/Pref-1 defines a subpopulation in the oval cell compartment of rat liver. *Gene Expr Patterns* 2004; **5**: 209-218

35 **Cimica V**, Batusic D, Chen Y, Hollemann T, Pieler T, Ramadori G. Transcriptome analysis of rat liver regeneration in a model of oval hepatic stem cells. *Genomics* 2005; **86**: 352-364

36 **Nakatsukasa H**, Nagy P, Evarts RP, Hsia CC, Marsden E, Thorgeirsson SS. Cellular distribution of transforming growth factor-beta 1 and procollagen types I, III, and IV transcripts in carbon tetrachloride-induced rat liver fibrosis. *J Clin Invest* 1990; **85**: 1833-1843

37 **So EC**, Wong KL, Huang TC, Tasi SC, Liu CF. Tetramethylpyrazine protects mice against thioacetamide-induced acute hepatotoxicity. *J Biomed Sci* 2002; **9**: 410-414

38 **De Groot H**, Sies H. Cytochrome P-450, reductive metabolism, and cell injury. *Drug Metab Rev* 1989; **20**: 275-284

39 **De Minicis S**, Candelaresi C, Marzioni M, Saccomano S, Roskams T, Casini A, Risaliti A, Salzano R, Cautero N, di Francesco F, Benedetti A, Svegliati-Baroni G. Role of endogenous opioids in modulating HSC activity in vitro and liver fibrosis in vivo. *Gut* 2008; **57**: 352-364

40 **Das SK**, Vasudevan DM. Alcohol-induced oxidative stress. *Life Sci* 2007; **81**: 177-187

41 **Lu Y**, Wang X, Cederbaum AI. Lipopolysaccharide-induced liver injury in rats treated with the CYP2E1 inducer pyrazole. *Am J Physiol Gastrointest Liver Physiol* 2005; **289**: G308-G319

42 **Kawada N**, Kristensen DB, Asahina K, Nakatani K, Minamiyama Y, Seki S, Yoshizato K. Characterization of a stellate cell activation-associated protein (STAP) with peroxidase activity found in rat hepatic stellate cells. *J Biol Chem* 2001; **276**: 25318-25323

43 **Tateaki Y**, Ogawa T, Kawada N, Kohashi T, Arihiro K, Tateno C, Obara M, Yoshizato K. Typing of hepatic nonparenchymal cells using fibulin-2 and cytoglobin/STAP as liver fibrogenesis-related markers. *Histochem Cell Biol* 2004; **122**: 41-49

44 **Kang JS**, Wanibuchi H, Morimura K, Puatanachokchai R, Salim EI, Hagihara A, Seki S, Fukushima S. Enhancement by estradiol 3-benzoate in thioacetamide-induced liver cirrhosis of rats. *Toxicol Sci* 2005; **85**: 720-726

45 **Asahina K**, Kawada N, Kristensen DB, Nakatani K, Seki S, Shiokawa M, Tateno C, Obara M, Yoshizato K. Characterization of human stellate cell activation-associated protein and its expression in human liver. *Biochim Biophys Acta* 2002; **1577**: 471-475

46 **Tièche S**, De Gottardi A, Kappeler A, Shaw S, Sägesser H, Zimmermann A, Reichen J. Overexpression of endothelin-1 in bile duct ligated rats: correlation with activation of hepatic stellate cells and portal pressure. *J Hepatol* 2001; **34**: 38-45

47 **Kuroda N**, Yamanaka J, Okada T, Hirano T, Iimuro Y, Fujimoto J. Hepatic effects of influxed endothelin-1 from portal vein: in situ portal vein infusion model using dogs. *J Hepatobiliary Pancreat Surg* 2006; **13**: 160-166

48 **Guo CY**, Wu JY, Wu YB, Zhong MZ, Lu HM. Effects of endothelin-1 on hepatic stellate cell proliferation, collagen synthesis and secretion, intracellular free calcium concentration. *World J Gastroenterol* 2004; **10**: 2697-2700

49 **Shibamoto T**, Kamikado C, Koyama S. Increased sinusoidal resistance is responsible for the basal state and endothelin-induced venoconstriction in perfused cirrhotic rat liver. *Pflugers Arch* 2008; **456**: 467-477

S- Editor Sun H **L- Editor** Ma JY **E- Editor** Li JY